Boletín de la Sociedad Española de Cerámica y Vidrio
Vol 51, 1, 1-6, Enero-Febrero 2012 ISSN 0366-3175. eISSN 2173-0431.
doi: 10.3989/cyv.012012

BOLETIN DE LA SOCIEDAD ESPAÑOLA DE
Cerámica y Vidrio
A R T I C U L O

Improvement of thermoelectric properties of $Bi_2Sr_2Co_{1.8}O_x$ through solution synthetic methods

M. A. TORRES[1], A. SOTELO[2], SH. RASEKH[2,*], I. SERRANO[2], G. CONSTANTINESCU[2], M. A. MADRE[2], J. C. DIEZ[2]

[1]Universidad de Zaragoza, Dpto. de Ingeniería de Diseño y Fabricación, C/María de Luna 3, 50018-Zaragoza (Spain).
[2]Instituto de Ciencia de Materiales de Aragón, ICMA (CSIC-Universidad de Zaragoza), Mª de Luna, 3. 50018 Zaragoza, Spain.

Several solution synthetic methods, sol-gel and a polymeric route, have been studied in order to obtain $Bi_2Sr_2Co_{1.8}O_x$ ceramics with improved thermoelectric properties, compared to the classical solid state reaction. The products obtained by these different methods have been compared using DTA-TGA, powder X-ray diffraction, scanning electron microscopy, and thermoelectric characterizations. All the samples obtained by solution synthesis show higher homogeneity and lower content of secondary phases. The main differences in thermoelectrical properties are due to the decrease of electrical resistivity in samples obtained by solution methods, compared with the solid state obtained samples. Between them, the decrease is especially high for those samples prepared by the polymer solution method. Therefore, the polymeric solution synthesis route is shown to yield a power factor four times higher than the obtained for the solid state and sol-gel methods at room temperature.

Keywords: Processing, Electrical properties, Microstructure, Thermopower, Cobaltites.

Mejora de las propiedades termoeléctricas de $Bi_2Sr_2Co_{1.8}O_x$ por métodos de síntesis en disolución

Se han obtenido cerámicas termoeléctricas $Bi_2Sr_2Co_{1.8}O_x$ utilizando varios métodos de síntesis, el clásico por estado sólido, sol-gel y de matriz polimérica. Se han comparado los productos obtenidos por las diferentes vías a través de técnicas de DTA-TGA, difracción de rayos X en polvo, microscopía electrónica de barrido y de caracterización termoeléctrica. Todas las muestras obtenidas por los métodos en disolución poseen una mayor homogeneidad y menor contenido de fases secundarias. La principal diferencia en las propiedades termoeléctricas es debida a la disminución de la resistividad eléctrica en las muestras obtenidas por medio de métodos en disolución, comparado con las que se obtienen por estado sólido. Entre ellas, la reducción de la resistividad es mucho mayor para las que se obtienen por el método de matriz polimérica. Además, los materiales obtenidos por este último método poseen un factor de potencia, a temperatura ambiente, cuatro veces mayor que el obtenido en las sintetizadas por los otros dos métodos estudiados.

Keywords: Procesamiento, Propiedades eléctricas, Microestructura, Poder termoeléctrico, Cobaltitas.

1. INTRODUCTION

Nowadays, thermoelectric (TE) materials with high efficiency are strongly required for electric power generation, in terms of waste heat recovery. Thermoelectric energy conversion has been shown as an effective technology that can be used to transform a thermal gradient between the cold and hot side of a thermoelectric system directly to a voltage difference. The conversion efficiency of these materials is quantified by a dimensionless factor, the figure of merit, ZT, defined as $TS^2/\rho\kappa$, where S is the Seebeck coefficient (or thermopower, TEP), ρ the electrical resistivity, κ the thermal conductivity, and T, the absolute temperature [1]. As a consequence, a high performing TE material should involve high thermopower and low resistivity, together with a low thermal conductivity.

From the discovery of high thermoelectric performances in the Na_xCoO_2 ceramic material [2], characterized by a high Z value and large thermopower, great efforts have been performed to explore new cobaltites with high thermoelectric performances. As a consequence, some other layered cobaltites, such as $[Ca_2CoO_3][CoO_2]_{1.62}$ and $[Bi_{0.87}SrO_2]_2[CoO_2]_{1.82}$ were found to exhibit good thermoelectric properties [3-5]. Moreover, they can operate at high temperature in air without degradation, as compared to the intermetallic thermoelectric compounds, increasing ZT values.

Crystallographically, these cobaltites are composed of two different layers, with an alternate stacking of a common conductive CdI_2-type CoO_2 layer, with a two-dimensional triangular lattice, and an insulating block layer, with the rock-salt-type (RS) structure. The two sublattices (RS block and CdI_2-type CoO_2 layer) possess common a- and c-axis lattice parameters and β angles but different b-axis length, causing a misfit along the b-direction [6-8] that gives their common name: misfit cobaltites.

In functional ceramics, the processing techniques have shown to have an important influence on the grain size and phase purity of the final products which lead to the modification of their physical properties [9]. Commonly, the initial powders are prepared using the classical solid state

reaction method, with several mixing, milling and calcination processes. Furthermore, typical materials show incomplete reaction, and compositional inhomogeneities. On the other hand, solution syntheses offer some advantages, compared with classical solid state process, as higher precursor homogeneity and smaller particle size, which can result on the reduction of inhomogeneities and, as a consequence, the improvement of their properties.

Other important point is raising from the different possible oxidation states of cobalt in the cobaltite structure (Co^{+3} and Co^{+4}). The relative proportion between them explains the values of the TEP measured in this system, as can be deduced from the Koshibae's expression [10], relating TEP to the fraction of Co^{4+} over the total amount of cobalt. In this case, the exploration of new synthetic methods is a very promising route in order to improve the TEP values by modifying the Co^{4+} proportion in the samples.

The aim of this work is developing reproducible preparation methods that yield optimum quality $Bi_2Sr_2Co_{1.8}O_x$ powders for using as bulk ceramics or as precursors for textured materials. It is presented a comparison between three different synthetic methods, the conventional solid-state synthesis, a sol-gel method and a versatile polymer solution synthesis route developed in our laboratory [11,12] for other layered ceramics.

2. EXPERIMENTAL

The initial $Bi_2Sr_2Co_{1.8}O_x$ powders used in this work were prepared by the following methods:

(i) *Solid-state reaction:* Bi_2O_3 (98%, Panreac), $SrCO_3$ (98.5%, Panreac), and Co_3O_4 (98%, Panreac) powders were ball-milled for 30 minutes at 300 rpm in an agate mortar. The resulting mixture was then placed in a furnace and heated slowly to 750 °C, where it was kept for *c.a.* 12 h, followed by furnace cooling. The so obtained powder was ground and heated again at 800 ºC for another 12 h, manually milled and uniaxially pressed at around 250 MPa in form of nearly square prisms (~3 x 3 x 14 mm^3). Finally, the compacts were sintered, under air, for 24 h at 810 ºC, with furnace cooling.

(ii) *Sol-gel method:* $Bi(NO_3)_3 \cdot 5H_2O$ (≥98 %, Aldrich), $SrCO_3$ (98.5 %, Panreac), and $Co(NO_3)_2 \cdot 6H_2O$ (98 %, Panreac) powders were suspended in distilled water. Concentrated HNO_3 (analysis grade, Panreac) was added dropwise into the suspension until it turned into a clear pink solution. Citric acid (99.5 %, Panreac), and ethylene glycol (99 %, Panreac), were added to this solution in the adequate proportions. Evaporation of the solvent was performed slowly (between 50 and 100 ºC) in order to decompose the nitric acid excess, which allows the polymerization reaction between ethylene glycol and citric acid, forming a pink gel. The dried product was then decomposed (slow self combustion) by heating at 350 ºC for 1 h. The decomposed solid was mechanically ground for 30 minutes and calcined at 750 and 800 °C for 12 h, with an intermediate grinding. As for the solid state reaction, sintering was performed, following uniaxial pressing, at 810 ºC for 24 h, under air, with furnace cooling.

(iii) *Polymer solution synthesis:* To a suspensión of $Bi(CH_3CO_2)_2$ (99.99 + %, Aldrich), $Sr(CH_3CO_2) \cdot 2H_2O$ (Reagent grade, Alfa Aesar), and $Co(CH_3CO_2)_2 \cdot 4H_2O$ (98 %, Panreac) powders in distilled H_2O, glacial acetic acid (ACS Reagent, Panreac) was added until a pink clear solution was formed. Polyethylenimine (PEI) (50 % aqueous, Aldrich) was added to the above solution, which turned darker immediately due to the nitrogen-metal coordination. After partial evaporation (~80 vol. %) of water and acetic acid in a rotary evaporator, concentrated solution, with a very high viscosity, was placed onto a hot plate until a very dark pink paste appeared. Further heating turned this paste to violet color, followed by a slow combustion with the release of brown fumes (nitrogen oxides). The resulting powder was milled and calcined at 750 and 800 ºC for ca. 12 h, with an intermediate milling, uniaxially pressed and sintered for 24 h at 810 ºC, under air, with a final furnace cooling.

Phase development and transformations have been studied using DTA-TGA between 50 and 1000 ºC under air with a heating rate of 10 ºC/min, and powder X-ray diffraction (XRD) utilizing a Rigaku D/max-B X-ray powder diffractometer (CuKα radiation) between 10 and 40 degrees. Microstructural characterization has been carried out by means of electron microscopy (SEM, JEOL 6000), provided with an energy dispersive spectroscopy (EDS) system. Micrographs of fractured sections have been recorded to observe the general grain distribution, while longitudinal polished sections of the samples have been observed to analyze the different phases. Image analysis has been performed in several micrographs using Digital Micrograph software in order to estimate the amount of the different phases. The evaluation of the samples porosity has been performed determining the apparent density, on at least four samples for each synthetic method. Due to their simple shape, they have been weighed in an analytical weighing scale (Sartorius TE124S, error ± 0.0001 g) and measured their dimensions using a micrometer (Mitutoyo Digimatic Micrometer, error ± 0.001 mm).

Electrical resistivity and thermopower, were simultaneously determined by the standard dc four-probe technique in a LSR-3 measurement system (Linseis GMBh). They were measured in the steady state mode and at temperatures ranging from 50

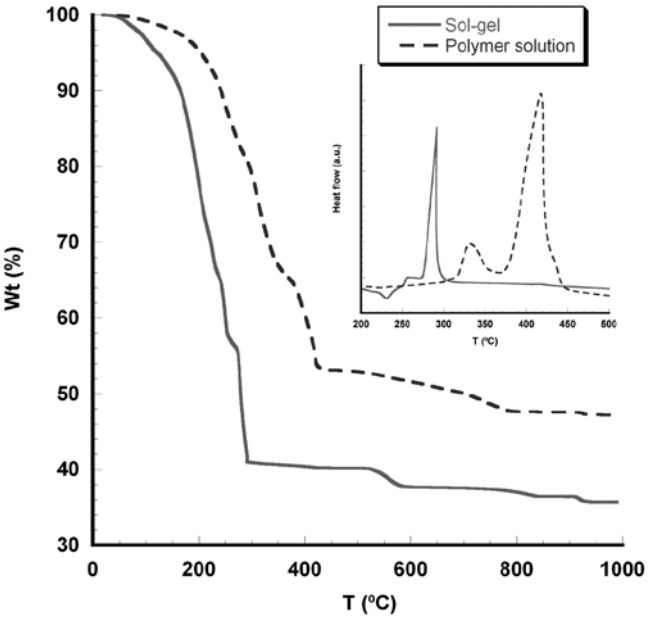

Figure 1. TGA plot vs. temperature of the initial solutions. The insert corresponds to the DTA data in the decomposition temperature range.

to 650 ºC under He atmosphere. With the electrical resistivity and thermopower data, the power Factor ($PF = S^2/\rho$) has been calculated in order to determine the samples performances. These electrical properties have been compared with the results reported in the literature at low temperatures (~50 ºC), where oxygen diffusion is negligible, avoiding the influence of the atmosphere on the compared values.

3. RESULTS AND DISCUSSION

3.1. Precursors characterization

A systematic study has been performed in order to obtain a deeper understanding of the processes taking place in each step of the materials processing for the different solution synthetic routes, and comparing them to the classical solid state method. In a first step, it is necessary to take into account the different cation coordination environments found for each solution method. Sol-gel method produces metal-oxygen coordination while metal-nitrogen coordination is formed in the polymer solution method. When studying the decomposition path of the coordination compounds obtained by the two solution methods by DTA-TGA (Fig. 1), clear differences can be observed between both of them. The main one is associated to the exothermic peaks found in DTA analysis (insert in Fig. 1). These exothermic peaks correspond to the organic materials decomposition (ethylene glycol + citric acid polymer for the sol-gel method and PEI for the polymer solution one) which leads to the coordination compounds destruction. The peaks appear at different temperatures for each synthetic method, higher for the polymer solution method than for the sol-gel one. This is a clear indication of the higher thermal stability of the metal-nitrogen coordination (found in the metal-PEI complex), compared with the metal-oxygen one (found in the sol-gel method). On the other hand, a single decomposition peak is observed for the sol-gel method while two peaks are found in the polymer method decomposition process. In order to understand this decomposition process, a small portion of the dry product obtained from the polymer solution has been heated on a hot plate under air until total decomposition of organic material. This process has shown that the decomposition is performed in two steps; the first one produces a very dense smoke (mainly composed of CO_2 and NO_x) [13] which tends to remain into the alumina crucible and, as a consequence, a highly reducing atmosphere can be found around the precursor powders (at temperatures around 300 ºC). After this step, slow combustion of the remaining organic material is produced (at 350-400 ºC), reaching temperatures around 700 ºC inside the crucible. This second step corresponds to the sharp peak appearing at about 420 ºC in the DTA plot (see insert in Fig.1).

After the slow combustion, it remains an open question with respect to the amount of metallic carbonates formed in this process and/or the organic materials in these powders. In order to determine their amount in these mixtures, DTA-TGA analyses were made between 450 and 1000 ºC (see Fig. 2) and compared with the initial mixture of oxides and carbonates (for the solid state route). As it can be observed in this figure, the polymer and sol-gel precursors start to decompose at lower temperatures than the solid state ones, which is associated to their smaller particle size, increasing their reactivity. On the other hand, precursors produced by solution methods show, approximately, the same weight loss and a little bit higher (~ 0.5%) than the precursors for the solid state route. This result indicates that, after decomposing the organic material, there is still a very small amount of organic material in these precursors.

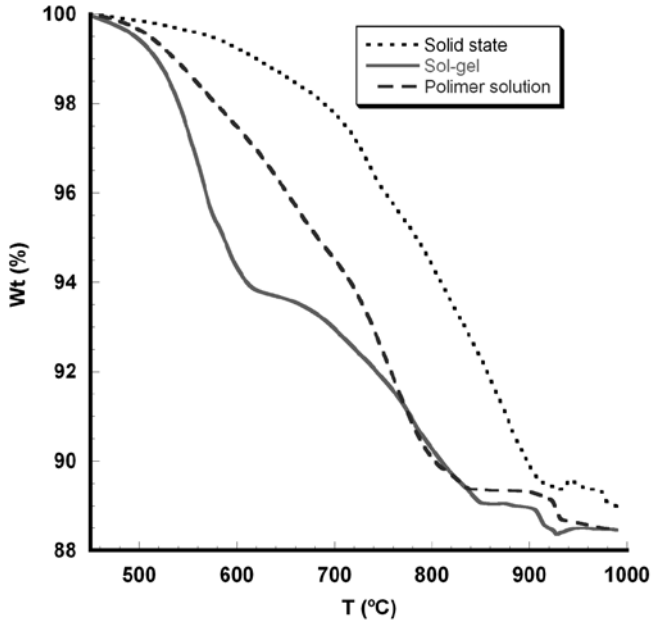

Figure 2. TGA plot vs. temperature of the sol-gel and polymer precursors after firing. The initial mixture of oxides and carbonates for the solid state method is represented for comparison.

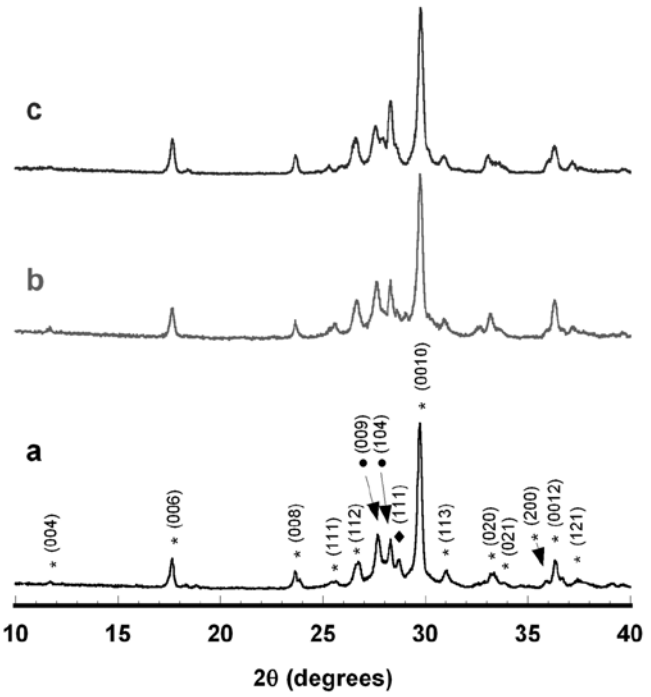

Figure 3. XRD plots of the sintered specimens obtained for the different synthetic methods. a) solid state, b) sol-gel, and c) polymer solution route. * indicates the thermoelectric $Bi_2Sr_2Co_{1.8}O_x$ phase, ● to the secondary $Bi_{0.75}Sr_{0.25}O_y$ non thermoelectric phase (R3mH'), and ♦ for Si (used as reference).

3.2. Sintered materials characterization

Powder XRD patterns for the different $Bi_2Sr_2Co_{1.8}O_x$ samples, after sintering at 800 ºC for 24 h, are displayed in Fig. 3. From this plot, it is clear that all the samples have very similar diffraction patterns and show minor peaks corresponding to non-thermoelectrical secondary phases. The highest peaks (marked with a *) belong to the misfit cobaltite phase and are in agreement with previously reported data [14]. Weak diffraction peaks are related to the non thermoelectric $Bi_{0.75}Sr_{0.25}O_y$ secondary phase (marked with a ●) with the ($R\bar{3}mH'$) space group [15], and ♦ indicates the Si (111) diffraction peak, used as reference. In this figure it can be seen a slight reduction on the $Bi_{0.75}Sr_{0.25}O_y$ peaks intensity which can be associated to a decrease on the secondary phase proportion from the solid state samples (Fig. 3a) to the polymer solution ones (Fig. 3c).

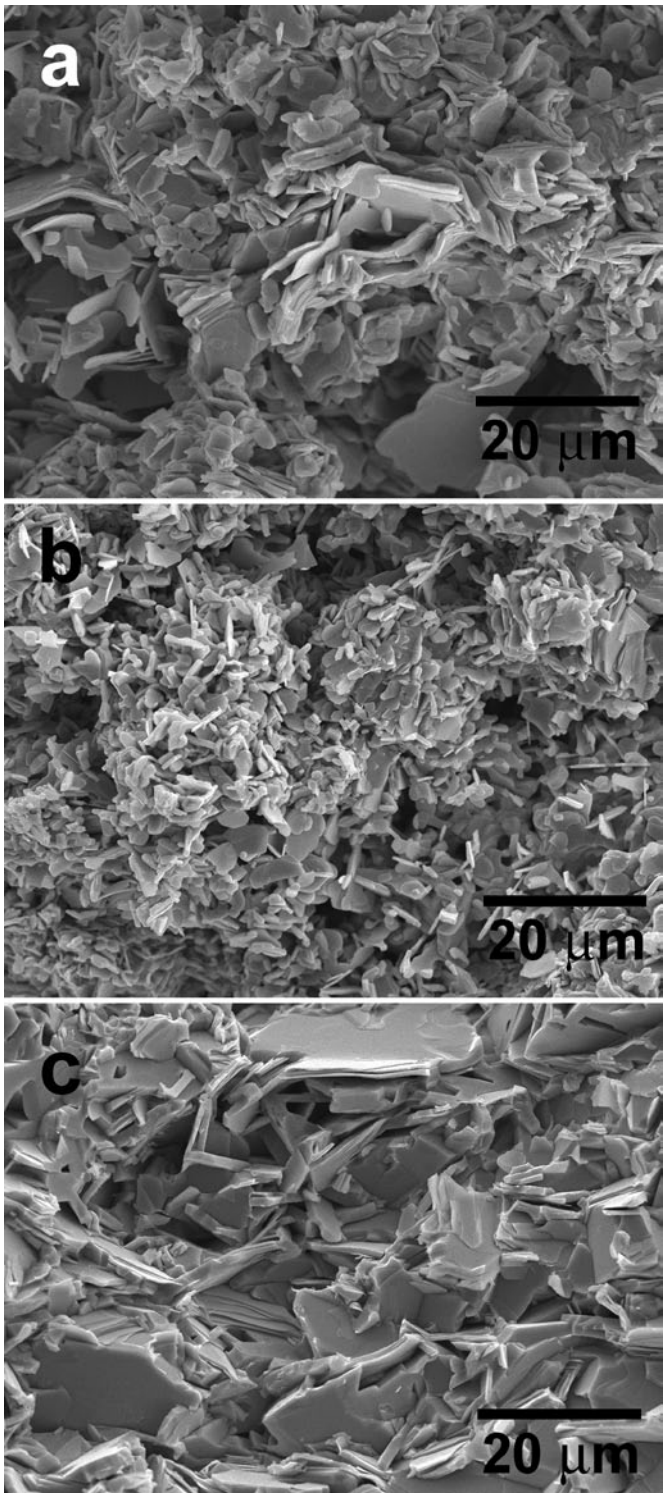

Figure 4. Scanning electron micrographs from transversal fractured samples obtained by: a) solid-state; b) sol-gel; and c) polymer reaction methods.

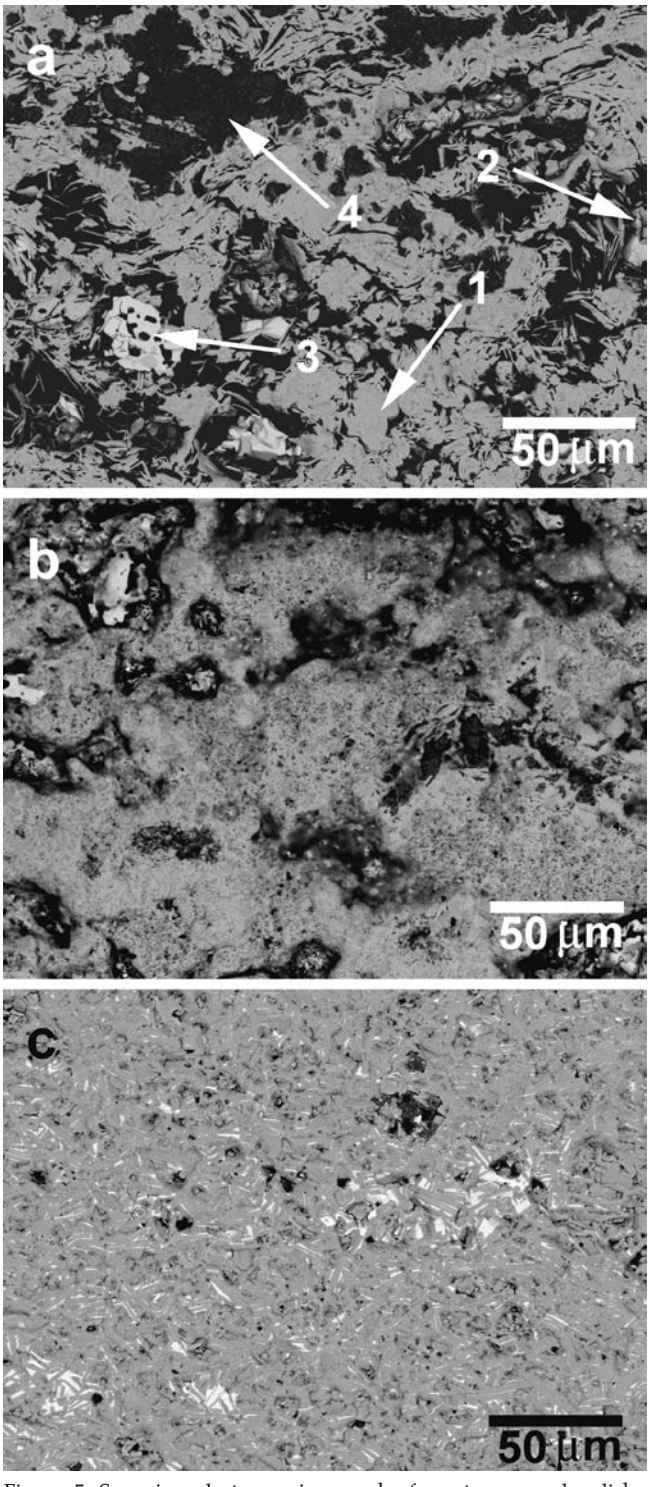

Figure 5. Scanning electron micrographs from transversal polished samples obtained by: a) solid-state; b) sol-gel; and c) polymer reaction methods. The different contrasts are numbered and correspond to 1) $Bi_2Sr_2Co_{1.8}O_x$; 2) SrO; 3) $Bi_{0.75}Sr_{0.22}O_y$; and 4) porosity.

SEM micrographs of the most representative transversal fractures for each sample are shown in Fig. 4. This figure clearly shows that samples derived from the solid state precursors (Fig. 4a) posses a broad grain size distribution while the sol-gel (Fig. 4b) and polymer (Fig. 4c) samples show more homogeneous particle sizes. On the other hand, sol-gel samples are formed by very small grains (see Fig. 4b), compared with the samples obtained by the other two synthetic methods while the polymer solution ones present the largest grains (more than 20 x 20 μm^2, Fig. 4c), as it was previously reported for $Bi_2Ca_2Co_{1.7}O_x$ ceramics [16] and in agreement with the results obtained in similar ceramic materials [17]. The grain sizes obtained with the polymer method are not common for solution routes but it can be explained by an increase in the enhanced precursors reactivity which can reduce sintering temperatures and times to obtain the final products [17]. From these images, the estimated grain thickness is around 0.2 μm but they are composed in turn, of a number of grains that are very thin and well stacked together. Due to the difficulty inherent to the determination of thickness of each individual grain by SEM observations, an estimation of their thickness has been performed from the XRD results applying Scherrer's formula using the (006) and (0010) diffraction peaks. The obtained mean value for the grain thickness is about 35 nm in all cases, which clearly indicates that the crystal preferential growth is produced along the ab plane.

When observing the transversal polished sections of the samples, displayed in Fig. 5, three different contrasts can be found. EDS analysis performed on different points for each contrast (numbered in Fig. 5 for clarity) showed that the grey one correspond to the thermoelectric $Bi_2Sr_2Co_{1.8}O_x$ phase (#1), dark grey to SrO (#2), white to $Bi_{0.75}Sr_{0.22}O_y$ (#3, very close to the $Bi_{0.75}Sr_{0.25}O_y$ composition, determined by XRD) and black to the porosity (#4). On the other hand, the amount of $Bi_{0.75}Sr_{0.22}O_y$ secondary phase is slightly decreasing from solid state (~ 4 vol.%, see Fig. 5a) to polymer solution (2 vol.%, see Fig. 5c) samples, also confirming the XRD results. Nevertheless, SrO phase has not been found on the XRD due to its relatively low proportion in the samples. Other important feature observed in this figure is that porosity is significantly decreased, compared with the solid state samples, when solution methods are used to synthesize the $Bi_2Sr_2Co_{1.8}O_x$ samples. The porosity is radically reduced for samples obtained by the polymer solution method.

In order to confirm this porosity evolution with the synthetic method, apparent density measurements were performed on at least four different sintered samples to get enough representative values. The density is increased from 63 ± 3 for the solid state samples, to 75 ± 2 for the sol-gel, and 91 ± 2 % of the theoretical density for the polymer solution method ones, which is in agreement with the SEM observations.

The temperature dependence of the electrical resistivity for samples obtained by the different synthetic methods is shown in Fig. 6. As it can be easily seen, the ρ(T) curves show a reduction of the resistivity values from the solid state obtained samples (around 87 mΩ.cm at 50 ºC), to the sol-gel ones (about 79 mΩ.cm at 50 ºC), and the polymer synthesized ones (approximately 21 mΩ.cm at 50 ºC). This evolution of the resistivity values is consistent with the reduction of the amount of the secondary phases observed in the SEM images and also with the apparent density values for all the samples. Furthermore, for samples obtained by the polymer solution method, ρ is nearly temperature independent and it is close to the values obtained for textured materials (~ 15 mΩ.cm at 275 ºC) [7] or single crystals (~ 18 mΩ.cm at room temperature) [14].

Fig. 7 displays the variation of TEP with temperature as a function of the synthetic method. The values are positive in the entire measured temperature range, indicating a dominating hole conduction mechanism. On the other hand, they increase almost linearly with temperature, with values of about 130 mV/K at ~ 50 ºC for all the samples, which are higher than those previously obtained for textured materials

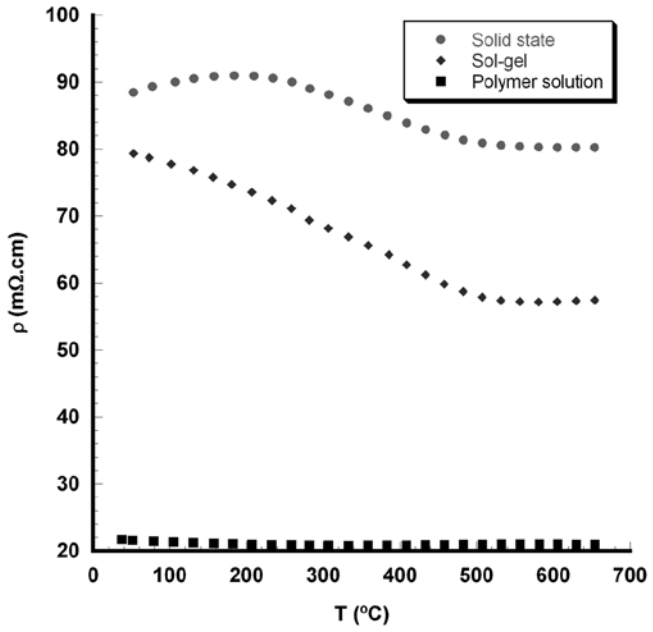

Figure 6. Temperature dependence of the electrical resistivity according to the synthetic method.

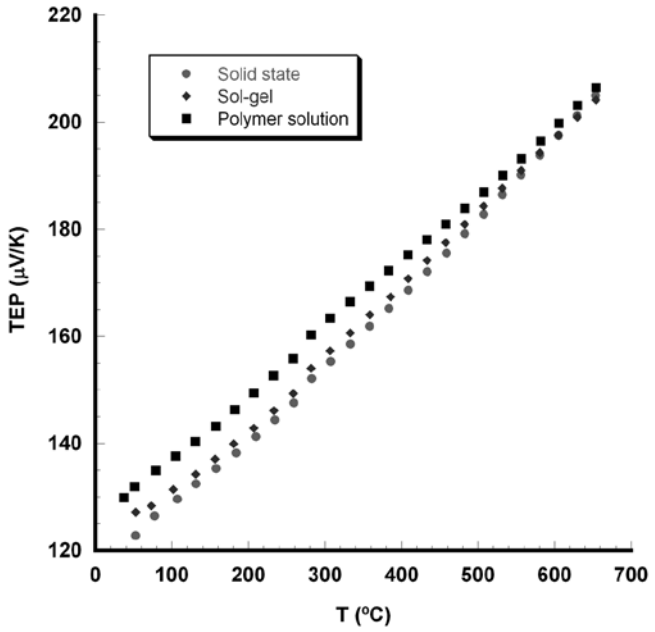

Figure 7. Temperature dependence of the thermopower according to the synthetic method.

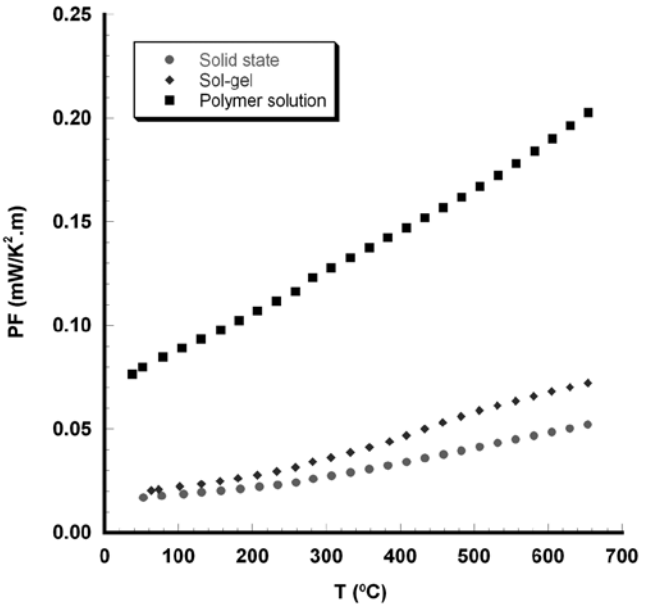

Figure 8. Temperature dependence of the power factor according to the synthetic method.

(125 mV/K at 275 ºC) [7] or single crystals (110 mV/K at room temperature) [14]. These values indicate that all the samples have, approximately, the same $Co^{+4}/(Co^{+3}+Co^{+4})$ proportion [10].

From the resistivity and TEP values, power factor has been calculated and is represented in Fig. 8, as a function of temperature for all the synthetic routes. From the data displayed in this figure, it is clear that polymer solution method highly improves PF values, compared with the obtained by classical solid state or sol-gel synthesis, in the whole range of measured temperatures. Moreover, when observing PF values obtained for the sample synthesized by the polymer solution method at room temperature (around 0.08 mW/K².m), it is higher than the obtained for single crystals (about 0.06 mW/K².m) [14], and even higher than the obtained for textured materials (approximately 0.10 mW/K².m at 275 ºC) [7] at the same temperature (around 0.12 mW/K².m).All the results showed in this work indicate that the PEI synthetic route is an adequate method to produce high quality and homogeneous Bi-Sr-Co-O ceramics. Moreover, when they are appropriately compacted and sintered, lead to bulk ceramics with improved thermoelectrical properties compared with previously reported data for single crystals or textured materials.

4. CONCLUSIONS

A comparison of several synthesis routes, solid-state, sol-gel and a polymer solution, to the $Bi_2Sr_2Co_{1.8}O_x$ phase has been performed. Solid-state and sol-gel synthetic methods result in a relatively good quality product, but the polymer solution method evaluated in this study provide much higher yields of the thermoelectric phase, together with a reduction of the ceramics porosity. As a consequence, this method has been revealed as the most advantageous, with respect to the decrease of the samples resistivity which leads to very high values of the power factor, about 300% of typical values for sintered materials, and even higher than the obtained for single crystals or textured materials.

ACKNOWLEDGEMENTS

This research has been supported by the Spanish Ministry of Science and Innovation-FEDER (Project MAT2008-00429). The authors wish to thank the Gobierno de Aragón (Consolidated Research Groups T12 and T87) for financial support; also to C. Gallego, C. Estepa and J. A. Gomez for their technical assistance.

REFERENCES

1. Thermoelectrics Handbook: Macro to Nano; D.M. Rowe, Ed.; CRC Press Taylor & Francis Group publications:Boca Raton, Fl. 2006; pp 1-3 to 1-7.
2. I. Terasaki, Y. Sasago, K. Uchinokura, Large thermoelectric power in $NaCo_2O_4$ single crystals, Phys. Rev. B 56, 20, 12685-12687 (1997).
3. R. Funahashi, I. Matsubara, H. Ikuta, T. Takeuchi, U. Mizutani, S. Sodeoka, An oxide single crystal with high thermoelectric performance in air, Jpn. J. Appl. Phys. 39, 11B, L1127-L1129 (2000).
4. A. C. Masset, C. Michel, A. Maignan, M. Hervieu, O. Toulemonde, F. Studer, B. Raveau, J. Hejtmanek, Misfit-layered cobaltite with an anisotropic giant magnetoresistance $Ca_3Co_4O_9$, Phys. Rev. B 62, 1, 166-175 (2000).
5. H. Leligny, D. Grebille, O. Perez, A. C. Masset, M. Hervieu, B. Raveau, A five-dimensional structural investigation of the misfit layer compound $[Bi_{0.87}SrO_2]_2[CoO_2]_{1.82}$, Acta Cryst. B 56, Part 2, 173-182 (2000).
6. A. Maignan, S. Hébert, M. Hervieu, C. Michel, D. Pelloquin, D. Khomskii, Magnetoresistance and magnetothermopower properties of Bi/Ca/Co/O and Bi(Pb)/Ca/Co/O misfit layer cobaltites, J. Phys.: Condens. Matter 15, 17, 2711-2723 (2003).
7. H. Itahara, C. Xia, J. Sugiyama, T. Tani, Fabrication of textured thermoelectric layered cobaltites with various rock salt-type layers by using beta-$Co(OH)_2$ platelets as reactive templates, J. Mater. Chem. 14, 1, 61-66 (2004).
8. E. Guilmeau, M. Mikami, R. Funahashi, D. Chateigner, Synthesis and thermoelectric properties of $Bi_{2.5}Ca_{2.5}Co_2O_x$ layered cobaltites, J. Mater. Res. 20, 4, 1002-1008 (2005).
9. Sh. Rasekh, M. A. Madre, A. Sotelo, E. Guilmeau, S. Marinel, J. C. Diez. Effect of synthetic method on the thermoelectrical properties of textured $Bi_2Ca_2Co_{1.7}O_x$ ceramics. Bol. Soc. Esp. Ceram. V. 49, 1, 89-94 (2010).
10. W. Koshibae, K. Tsuitsui, S. Maekawa, Thermopower in cobalt oxides, Phys. Rev. B 62, 11, 6869-6872 (2000).
11. G. F. de la Fuente, A. Sotelo, Y. Huang, M. T. Ruiz, A. Badia, L. A. Angurel, F. Lera, R. Navarro, C. Rillo, R. Ibañez, D. Beltran, F. Sapiña and A. Beltran, Polymer solution processing of (Bi, Pb)-Sr-Ca-Cu-O, Physica C 185-189, 509-510 (1991).
12. A. Sotelo, L. A. Angurel, M. T. Ruiz, A. Larrea, F. Lera, G. F. de la Fuente, Stoichiometry variation effect on the superconducting properties of polymer-processed $(Bi_{1-x}Pb_x)_2Sr_2Ca_2Cu_3O_{10}$ ceramics, Solid State Ionics 63-65, 883-888 (1993).
13. A. Sotelo, G. F. de la Fuente, F. Lera, D. Beltran, F. Sapiña, R. Ibañez, A. Beltran, M. R. Bermejo. Novel polymer solution synthesis of the 110K superconducting phase in the bismuth system. Chem. Mater. 5, 851-856 (1993).
14. T. Itoh, I. Terasaki, Thermoelectric properties of $Bi_{2.3-x}Pb_xSr_{2.6}Co_2O_y$ single crystals, Jpn. J. Appl. Phys. 39, 12A, 6658-6660 (2000).
15. D. Mercurio, J. C. Champarnaud-Mesjard, B. Frit, P. Conflant, J. C. Boivin, T. Vogt, Thermal evolution of the crystal structure of the rhombohedral $Bi_{0.75}Sr_{0.25}O_{1.375}$ phase: a single crystal neutron diffraction study, J. Solid State Chem. 112, 1, 1-8 (1994).
16. A. Sotelo, Sh. Rasekh, M. A. Madre, E. Guilmeau, S. Marinel, J. C. Diez, Solution-based synthesis routes to thermoelectric $Bi_2Ca_2Co_{1.7}O_x$, J. Eur. Ceram. Soc. 31, 1763-1769 (2011).
17. V. Garnier, R. Caillard, A. Sotelo, G. Desgardin. Relationship among synthesis, microstructure and properties in sinter-forged Bi-2212 ceramics. Physica C 319, 197-208 (1999).

Recibido: 25/06/2011
Aceptado: 21/10/2011